Weyl semimetal

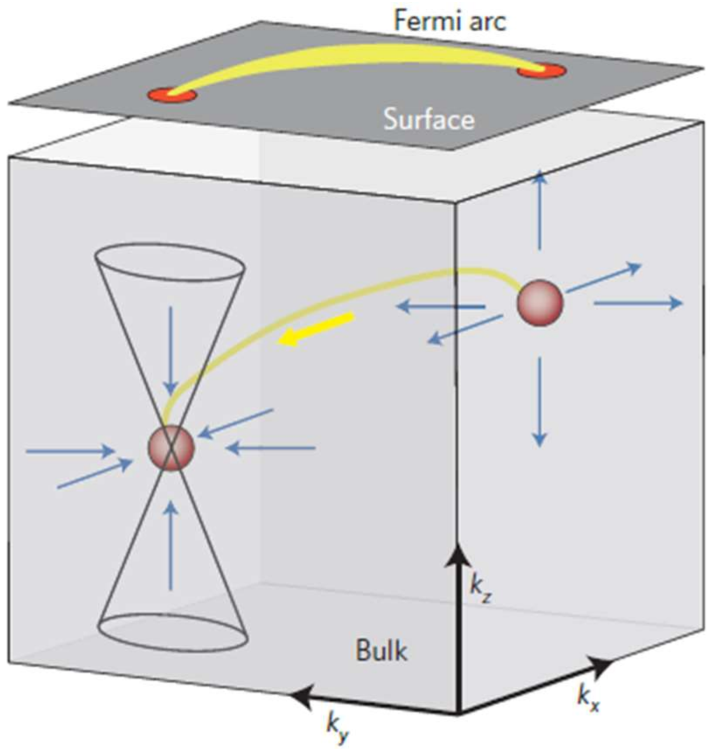

Band theory of solids

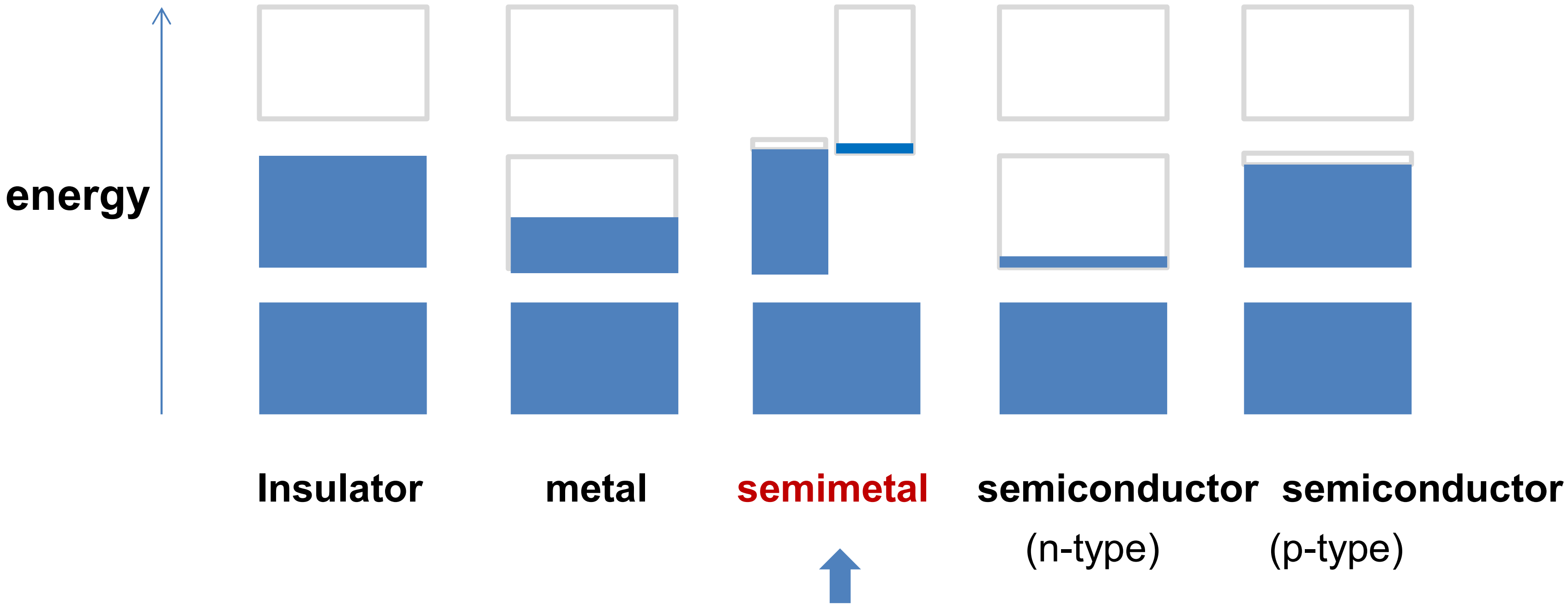

Small DOS near Fermi level.

Graphene as a 2D semi-metal.

3D analogue of graphene?

→ Weyl semimetal

Accidental degeneracy between 2 levels (2D, 3D)

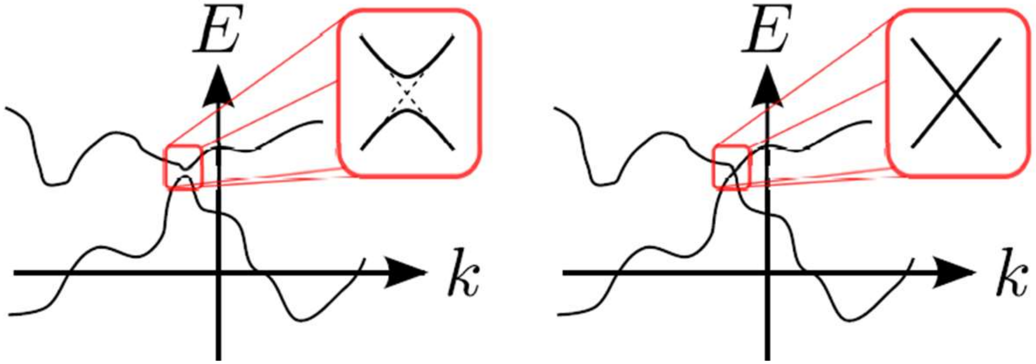

Avoided crossing | Crossing

Fig. from Meng's thesis

- Wigner-von Neumann "theorem" (1929):

  2-level *H* can be expanded by Pauli matrices,

$$H = d_0(\vec{k}) + d_x(\vec{k})\sigma_x + d_y(\vec{k})\sigma_y + d_z(\vec{k})\sigma_z$$

$$\rightarrow E_\pm = d_0 \pm \sqrt{d_x^2 + d_y^2 + d_z^2}$$

$\rightarrow$ degeneracy only when $d_x = d_y = d_z = 0$

(Co-dimension is 3)

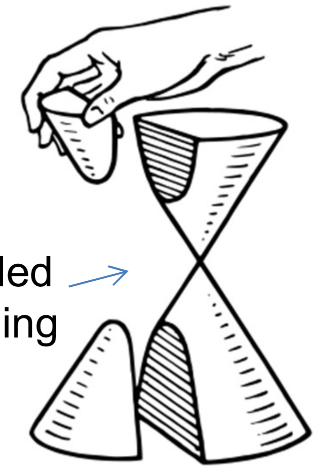

- 3D: one (or several) point degeneracy in 3D ***k***-space
- 2D: unlikely to have a point degeneracy in 2D ***k***-space

Stability of the Dirac point in graphene

- TRS $$H(\vec{k})^* = H(-\vec{k})$$ $$\rightarrow d_x(\vec{k}), d_y(\vec{k}), d_z(\vec{k}) = \text{even, odd, even}$$

- SIS (for graphene, $\pi=\sigma_x$)

$$\sigma_x H(\vec{k})\sigma_x = H(-\vec{k})$$
$$\rightarrow d_x(\vec{k}), d_y(\vec{k}), d_z(\vec{k}) = \text{even, odd, odd}$$

TRS+SIS $\rightarrow$ no σ_z term ← Co-dimension is 2
(point degeneracy in 2D BZ)

- point degeneracy is further protected by C_3 symmetry (Ch 7, Bernevig)

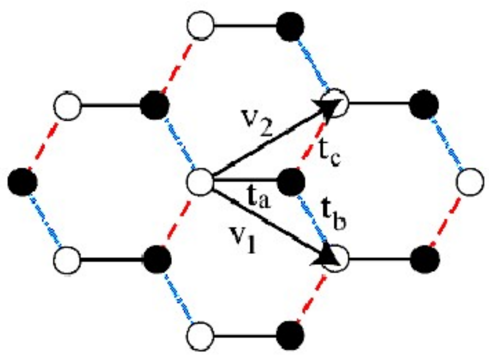

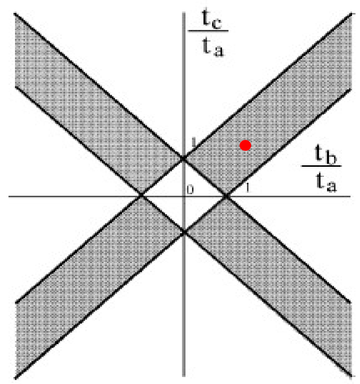

Hasegawa et al, PRB 2006

Consequence of level crossing

- 2 level crossing in 2D (SS of TI, graphene)

e.g., $\mathrm{H}_{SS} = \alpha(\boldsymbol{\sigma} \times \mathbf{k})_z + O(k^2)$

$$\Rightarrow \quad F_z^{\pm} = \mp\pi\delta^2(\mathbf{k})$$

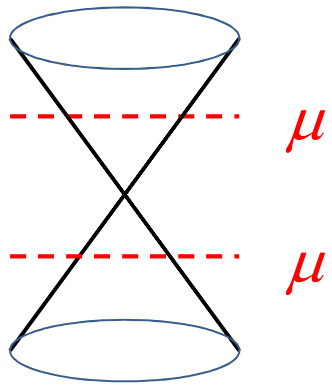

- 2 level crossing in 3D (Weyl semi-metal)

e.g., $H_{2\times 2}(\vec{k}) = \vec{k} \cdot \vec{\sigma}$

$$\Rightarrow \quad \vec{F}_{\pm} = \mp\frac{1}{2}\frac{\hat{k}}{k^2}$$

(Recall the Berry curvature of Zeeman coupling)

A Weyl point is a "monopole" in momentum space

(source or sink of Berry flux)

Chirality and monopole charge

- Near a Weyl point

$$H_{2\times 2}(\vec{q}) = h_0(\vec{q}) + \vec{h}(\vec{q})\cdot\vec{\sigma}, \qquad \vec{q} \equiv \vec{k}_0 + \vec{k}$$

$$\simeq h_0(\vec{q}) + \vec{h}\left(\vec{k}_0\right)\cdot\vec{\sigma} + \underbrace{\frac{\partial h_i}{\partial k_j} k_j\,\sigma_i}_{= \vec{v}_i\cdot\vec{k}\,\sigma_i}$$

手徵 Chirality (or helicity)

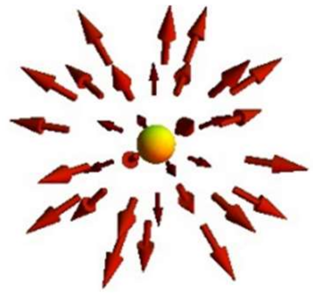

$\chi = +$

$$\chi \equiv \mathrm{sgn}\left[\det\left(\frac{\partial h_i}{\partial k_j}\right)\right] \text{ or } \mathrm{sgn}(\vec{v}_1\cdot\vec{v}_2\times\vec{v}_3)$$

$$\text{e.g.,} \qquad H = \pm v_F \vec{k}\cdot\vec{\sigma}, \qquad \chi = \pm$$

Berry curvature

$$\vec{F}_{-}^{\chi} = \frac{\chi}{2}\frac{\hat{k}}{k^2}$$

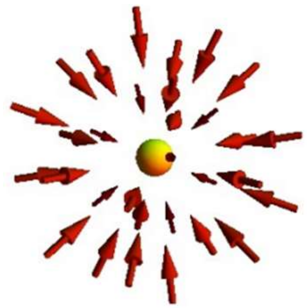

$\chi = -$

- Berry flux (~monopole charge) is quantized

$\Phi_F = 2\pi C_1$.

Stability of Weyl point

Weyl point is stable against perturbation

$$H = \pm v_F \vec{\sigma} \cdot \vec{k} + H'$$

a general perturbation:
$H' = a(\vec{k}) + \vec{b}(\vec{k}) \cdot \vec{\sigma}$

$$\rightarrow H' \cong a(\vec{k}) + \vec{b}(0) \cdot \vec{\sigma} + \frac{\partial b_i(0)}{\partial k_j} k_j \sigma_i$$

Shift position of node

Renormalize v_F

e. g., $H = v_F \vec{\sigma} \cdot \vec{k} + m\sigma_z$

- Weyl node can only appear/disappear by pair creation/annihilation

Nielsen-Ninomiya theorem (1981): 二宫正夫

Aka Fermion-doubling theorem, no-go theorem

In a lattice, massless Weyl fermions must appear in pairs with opposite chiralities.

- Energy band in 1D BZ

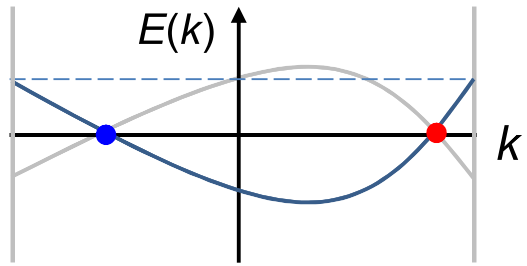

Zeros need to appear in pairs

- Energy band in 3D BZ

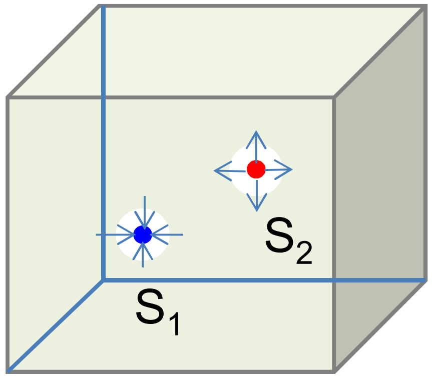

Total Berry flux from Weyl points needs to be zero.

To be precise, for a lattice in odd space dimensions, without breaking any of these: translation symmetry, chiral symmetry (locality, hermiticity), massless Weyl fermions must appear in pairs.

Note: 1. Used to be a problem in lattice QCD

2. In 2 dim, chirality is not well-defined. E.g., graphene

Topological origin of the Nielsen-Ninomiya theorem

Winding number again

Index of a point defect in a vector field

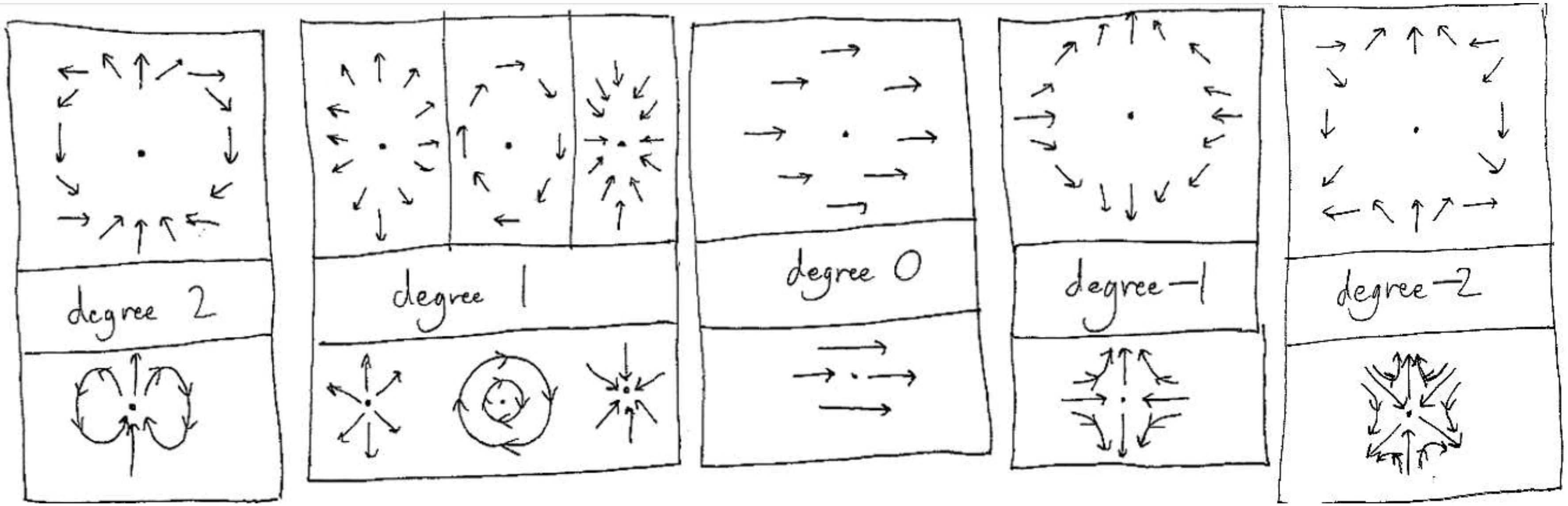

Fig from Jonas Kibelbek

Hopf-Poincare theorem

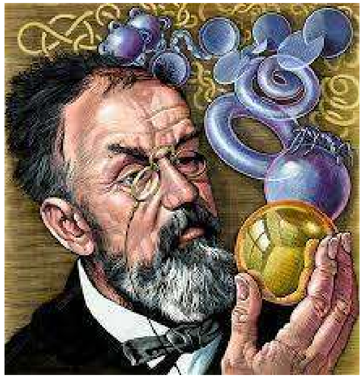

- Connecting index of point defect with topology

$$\sum_i ind(v_i) = \chi(M)$$

Euler characteristics

For a sphere

$$\sum_i ind(v_i) = 2$$

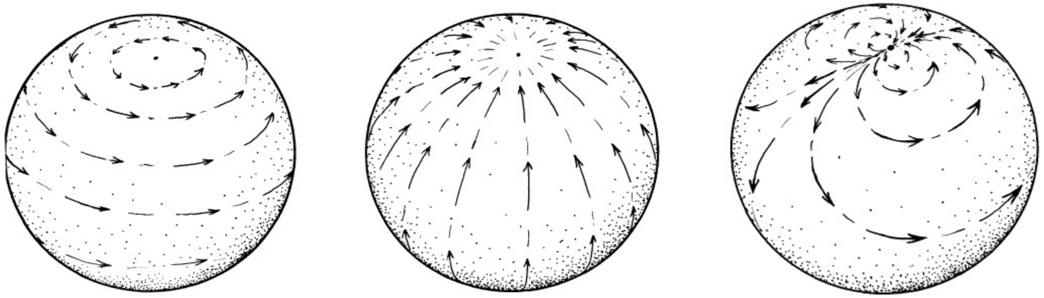

For a torus

$$\sum_i ind(v_i) = \chi(T^2) = 0$$

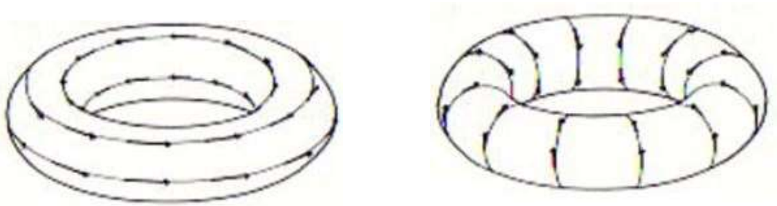

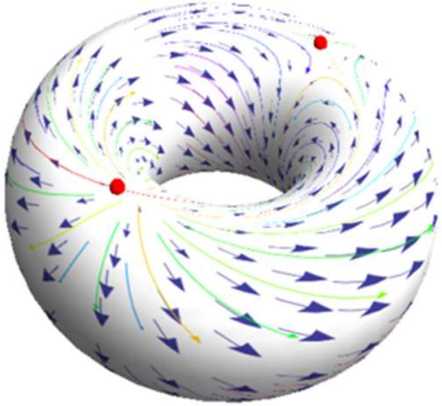

Brillouin zone as a torus (1D, 2D, 3D)

Berry connection **A**(***k***) as a vector field in BZ

Symmetry and Weyl point

$$H = \pm v_F \vec{\sigma} \cdot (\vec{k} - \vec{k}_0)$$

A monopole at $\boldsymbol{k}_0$

- TR Symm

$$\vec{k} \to -\vec{k}, \quad \vec{\sigma} \to -\vec{\sigma}$$

$$H \to H' = \pm v_F \vec{\sigma} \cdot \left(\vec{k} + \vec{k}_0\right)$$

→ A monopole at $-\boldsymbol{k}_0$ with the *same* chirality

- SI Symm

$$\vec{k} \to -\vec{k}, \quad \vec{\sigma} \to \vec{\sigma}$$

$$H \to H' = \mp v_F \vec{\sigma} \cdot \left(\vec{k} + \vec{k}_0\right)$$

→ A monopole at $-\boldsymbol{k}_0$ with the *opposite* chiralities

- Nielsen-Ninomiya theorem: always a pair with *opposite* chirality

TRS	IS	Implications	Min. number
×	×	Weyl nodes can be at any $\vec{k}$ and may have different energies.[113]	2
✓	×	Weyl node at $\vec{k}_0 \Leftrightarrow$ Weyl node of *same* chirality at $-\vec{k}_0$.	4
×	✓	Weyl node at $\vec{k}_0 \Leftrightarrow$ Weyl node of *opposite* chirality at $-\vec{k}_0$.	2
✓	✓	Not topologically stable	none

↖ Dirac point (but can be protected by crystal symmetry)

Meng T thesis 2012

Families of fermions in Particle physics

Realizations in Solid-state

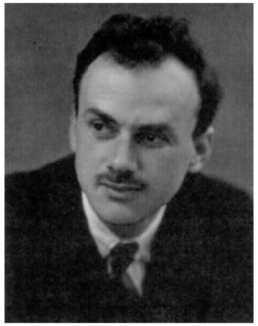

- Dirac fermion (1928)
  - Relativistic spin ½ fermion
  - 4 components
  - Electron, proton …

$$\begin{pmatrix} \varphi_1 \\ \varphi_2 \\ \varphi_3 \\ \varphi_4 \end{pmatrix}$$

Graphene with spin (2004)

- Weyl fermion (1929)
  - Massless ½ fermion
  - 2 components
  - Not found in nature

$$\begin{pmatrix} \varphi_1 \\ \varphi_2 \end{pmatrix}$$

TaAs… 砷化鉭 (2015)

- Majorana fermion (1937)
  - Being its own anti-particle
  - 2 *independent* components
  - Candidate for neutrino

$$\begin{pmatrix} \varphi_1 \\ \varphi_2 \\ \varphi_1^* \\ \varphi_2^* \end{pmatrix}$$

Semi-SC hybrid structure (2012, 14, 16)

From Dirac SM to Weyl SM

Break SIS　　Break TRS

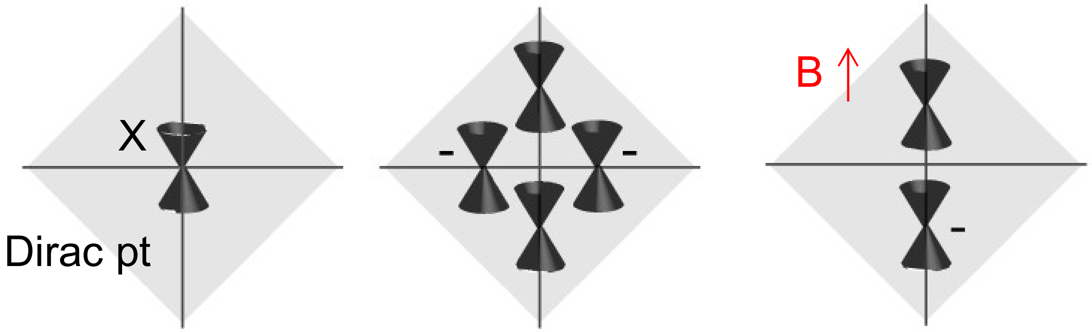

Not topo stable

Young et al, PRL 2012

Searching for degenerate point

1. Band-inversion mechanism (e.g., Na_3Bi, Cd_3As_2)

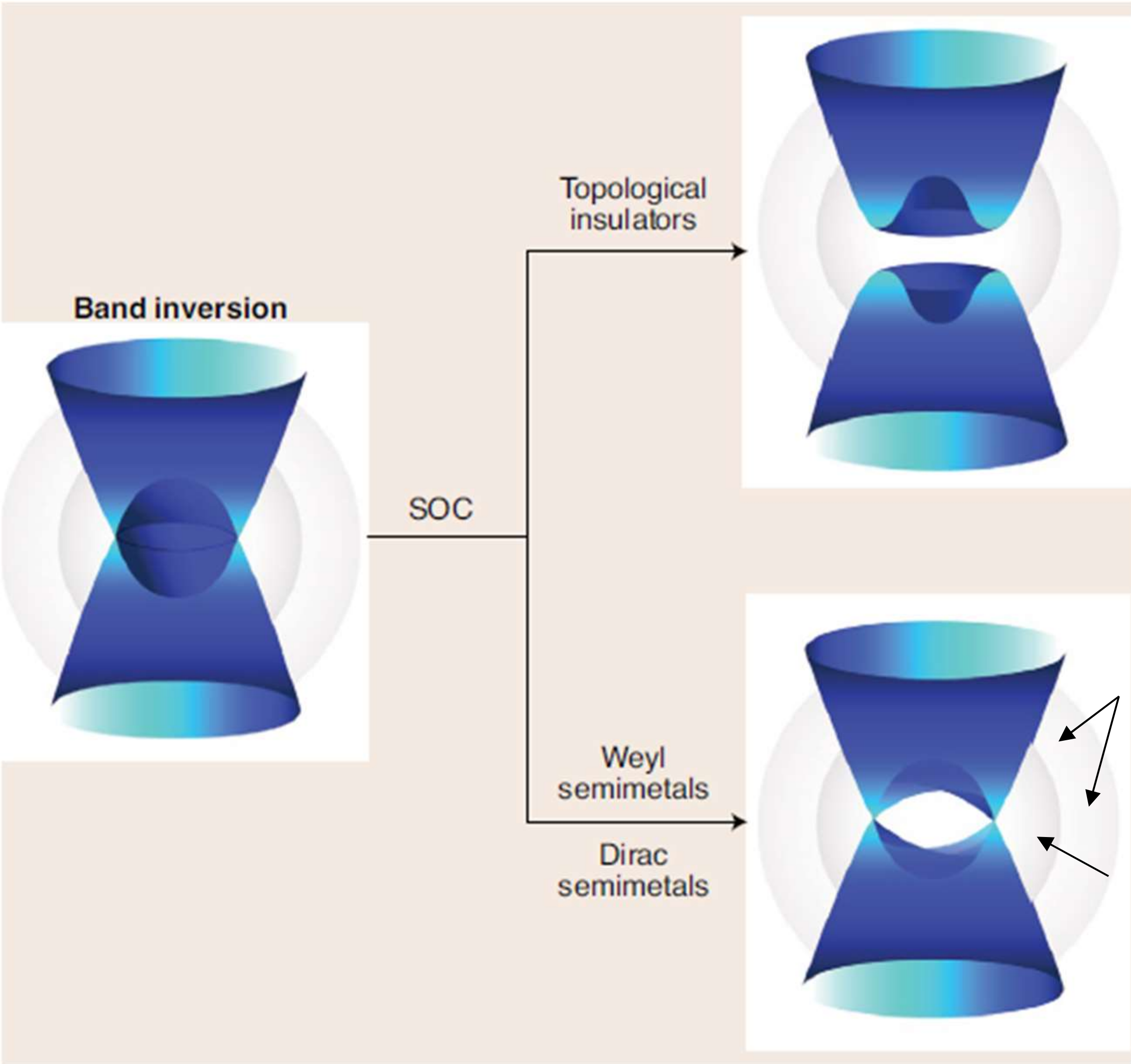

Fig: Narang et al, Nat Mater 2021

- **Avoided crossing due to coupling of 2 bands**

Along some symm axis:

- **2 branches from different IRs (with different symm eigenvalues, no coupling) of the symmetry.**
- **Dirac point could disappear if band-inversion is tuned away (symmetry unchanged)**

2. Symmetry-enforced mechanism (e.g., $PdTe_2$, $PtTe_2$, $PtSe_2$)

Search for space group that supports small groups $G_{\boldsymbol{k}}$ with 4-dim IR (FDIR)

- Possibility can be excluded for symmorphic space groups in 3D

  (see Armitage's RMP, 2018) 共型空間群

- Search within nonsymmorphic groups (i.e., with glide planes, screw axes)
- DPs usually are located on BZ boundary (face, edge, or corner)

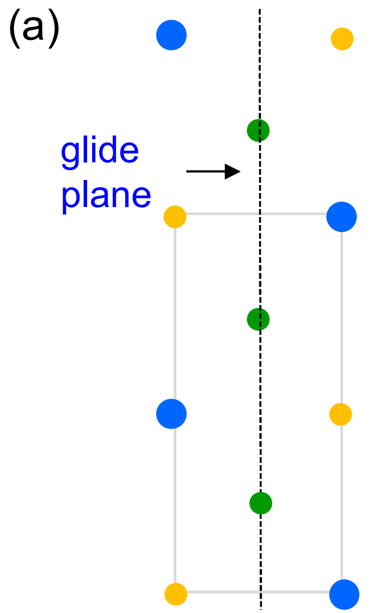

Reflection and glide

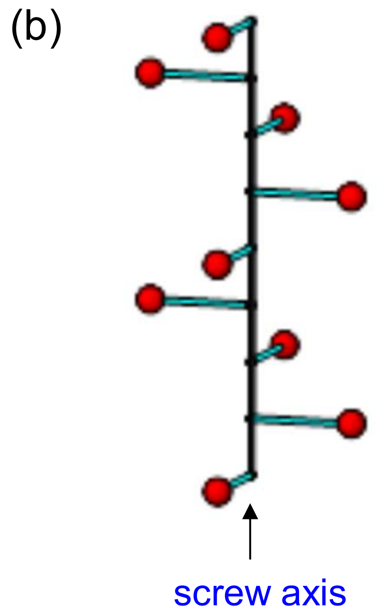

translation and screw

CRYSTALLOGRAPHY	d=2	d=3
LATTICES	5	14
POINT GROUPS	10	32
SPACE GROUPS	17	230
SYMMORPHIC	13	73
NON-SYMMORPHIC	4	157

[†] Of the 157 nonsymmorphic three-dimensional space groups, 155 involve glide planes or screw axes, and two are exceptional cases.

From the 32 point groups and the different Bravais lattices, we can get 73 space groups which involve ONLY rotations, reflection and rotoinversions.

Non-symmorphic space groups involve translational elements (screw axes and glide planes).
There are 157 non-symmorphic space groups

230 space groups in total!

Transition metal monopnictide 磷族

- With nonsymmorphic space group
- DP → WP by breaking SIS

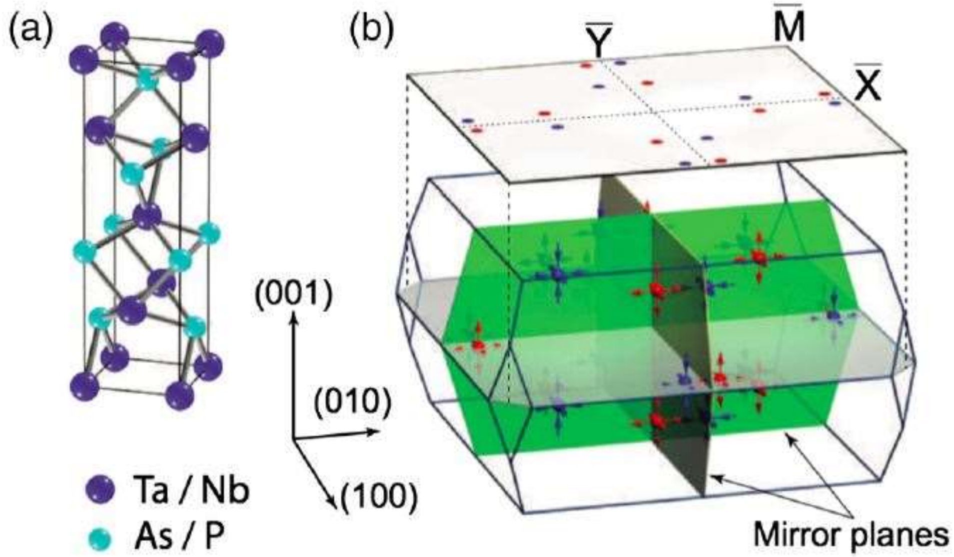

24 Weyl nodes

Huang et al, Nature Comm 2015

Physics related to Weyl fermions

1. Anomalous Hall effect
2. Fermi arc of surface state
3. Chiral anomaly
4. Chiral magnetic effect
5. …

Use
Burkov-Balent model
as an example

WP as a critical point of QPT:

Burkov-Balent model - multi-layer heterostructure

(Burkov and Balent PRL 2011)

Normal insulator
Topological insulator

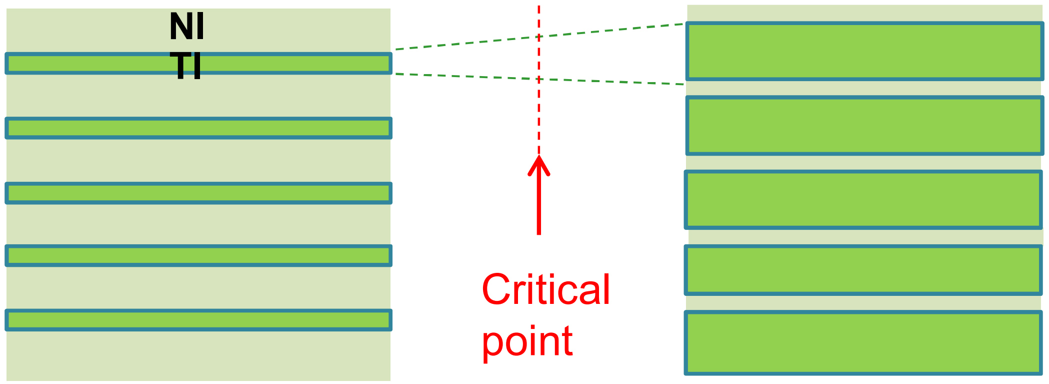

Coupling between surface states:

$t_s > t_d$: **normal insulator**

$t_s < t_d$: **topological insulator**

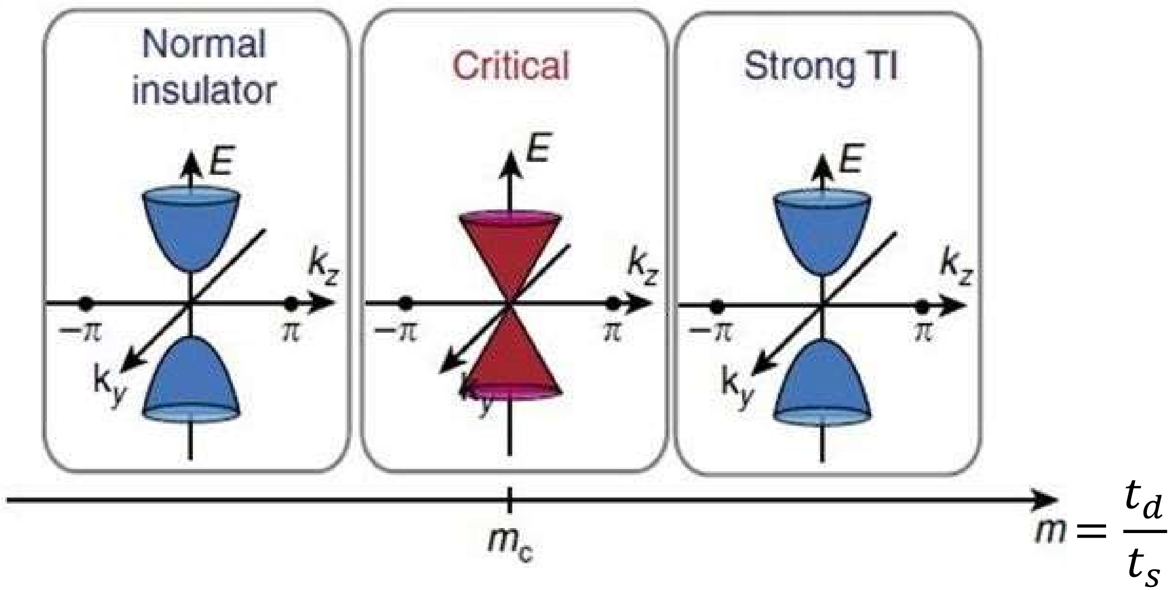

Two SS's from one TI slab

$$\mathsf{H} = v\tau_z \otimes (\boldsymbol{\sigma} \times \mathbf{k}_\perp) \cdot \hat{z} + m1 \otimes \sigma_z + t_s \tau_x \otimes 1$$

Multiple layers

$$\begin{aligned}\hat{\mathsf{H}} &= \sum_l \left[v\tau_z(\boldsymbol{\sigma} \times \mathbf{k}_\perp) \cdot \hat{z} + m\sigma_z + t_s\tau_x\right] c_l^\dagger c_l \\ &+ \sum_l t_d(\tau_+ c_l^\dagger c_{l+1} + \tau_- c_l^\dagger c_{l-1}),\end{aligned}$$

$$\tau_\pm = (\tau_x \pm i\tau_y)/2,\ c_l = (c_{lu}, c_{ld})^T$$

Fourier transform

$$c_l^\dagger = \frac{1}{\sqrt{N}} \sum_{k_z} e^{ildk_z} c_{k_z}^\dagger$$

$$\begin{aligned}\Rightarrow \hat{\mathsf{H}} &= \sum_{k_z} \Big[v\tau_z(\boldsymbol{\sigma} \times \mathbf{k}_\perp) \cdot \hat{z} c_{k_z}^\dagger c_{k_z} \\ &+ m\sigma_z c_{k_z}^\dagger c_{k_z} \\ &+ t_s \tau_x c_{k_z}^\dagger c_{k_z} \\ &+ t_d(e^{-ik_z d}\tau_+ c_{k_z}^\dagger c_{k_z} + e^{ik_z d}\tau_- c_{k_z}^\dagger c_{k_z}) \Big] \\ &= \sum_{k_z} \begin{pmatrix} \mathsf{h}_0 + m\sigma_z & t_s + t_d e^{-ik_z d} \\ t_s + t_d e^{ik_z d} & -\mathsf{h}_0 + m\sigma_z \end{pmatrix} c_{k_z}^\dagger c_{k_z} \\ &\equiv \sum_{k_z} \mathsf{H}_{k_z} c_{k_z}^\dagger c_{k_z},\end{aligned}$$

Each k_z is an independent subsystem

$$\begin{aligned}\mathsf{H}_{k_z} &= \tau_z \mathsf{h}_0 + m\sigma_z \\ &+ t_s\tau_x + t_d(e^{-ik_z d}\tau_+ + e^{ik_z d}\tau_-)\end{aligned}$$

$$\mathsf{h}_0 = v(\boldsymbol{\sigma} \times \mathbf{k}_\perp) \cdot \hat{z}$$

Unitary rotation

$$\mathsf{U} = \begin{pmatrix} 1 & 0 \\ 0 & \sigma_z \end{pmatrix}$$

$$\begin{aligned}\tau_{x,y} &\to \mathsf{U}^\dagger \tau_{x,y} \mathsf{U} = \tau_{x,y}\sigma_z, \\ \sigma_{x,y} &\to \mathsf{U}^\dagger \sigma_{x,y} \mathsf{U} = \tau_z \sigma_{x,y}.\end{aligned}$$

$$\Rightarrow \quad \begin{aligned}\mathsf{H}_{k_z} &= \mathsf{h}_0 + m\sigma_z \\ &+ [t_s\tau_x + t_d(e^{-ik_z d}\tau_+ + e^{ik_z d}\tau_-)]\sigma_z\end{aligned}$$

$$\begin{aligned}\mathsf{H}_{k_z} &= \mathsf{h}_0 + \underbrace{\left[m + \tau_z\sqrt{t_s^2 + t_d^2 + 2t_s t_d \cos(k_z d)}\right]}_{M_{\tau_z}(k_z)}\sigma_z \\ &= v(\boldsymbol{\sigma} \times \mathbf{k}_\perp) \cdot \hat{z} + M_{\tau_z}(k_z)\sigma_z,\end{aligned}$$

Band structure

$$\varepsilon_{\pm}^{\tau_z} = \pm\sqrt{v^2(k_x^2+k_y^2)+M_{\tau_z}^2(k_z)}$$

$$M_{\tau_z}(k_z) = m + \tau_z\sqrt{t_s^2+t_d^2+2t_st_d\cos(k_zd)}$$

Gap closes when

$$\cos(k_0d) = \frac{m^2-(t_s^2+t_d^2)}{2t_st_d}$$

$$\underbrace{|t_s-t_d|}_{m_{c1}} \le m \le \underbrace{|t_s+t_d|}_{m_{c2}}$$

Hall conductivity

$$\sigma_H^{3D} = \frac{1}{L_z}\sum_{k_z}\sigma_H^{2D}(k_z)$$
$$= \int_{-\pi/d}^{\pi/d}\frac{dk_z}{2\pi}\sigma_H^{2D}(k_z) = \frac{e^2}{h}\frac{\bar{k}_0}{\pi}$$

Semi-quantized Hall conductivity

$$\sigma_H^{3D} = \frac{e^2}{h}\frac{1}{d}$$

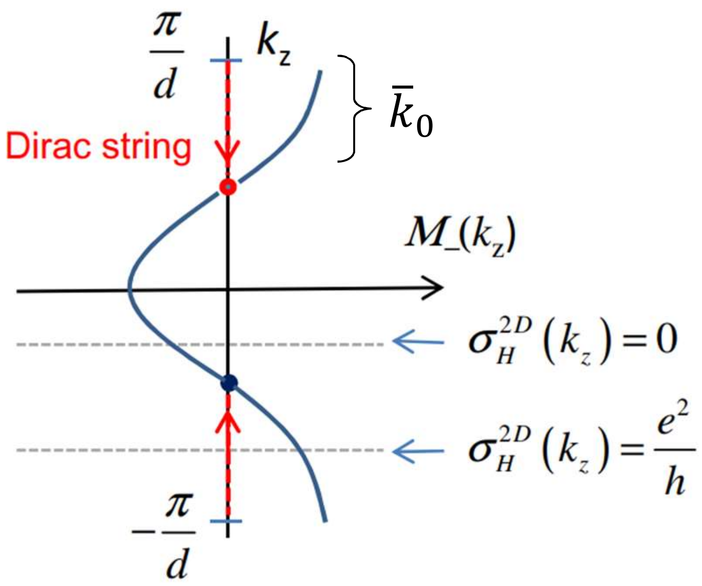

Phase diagram of Burkov-Balent model

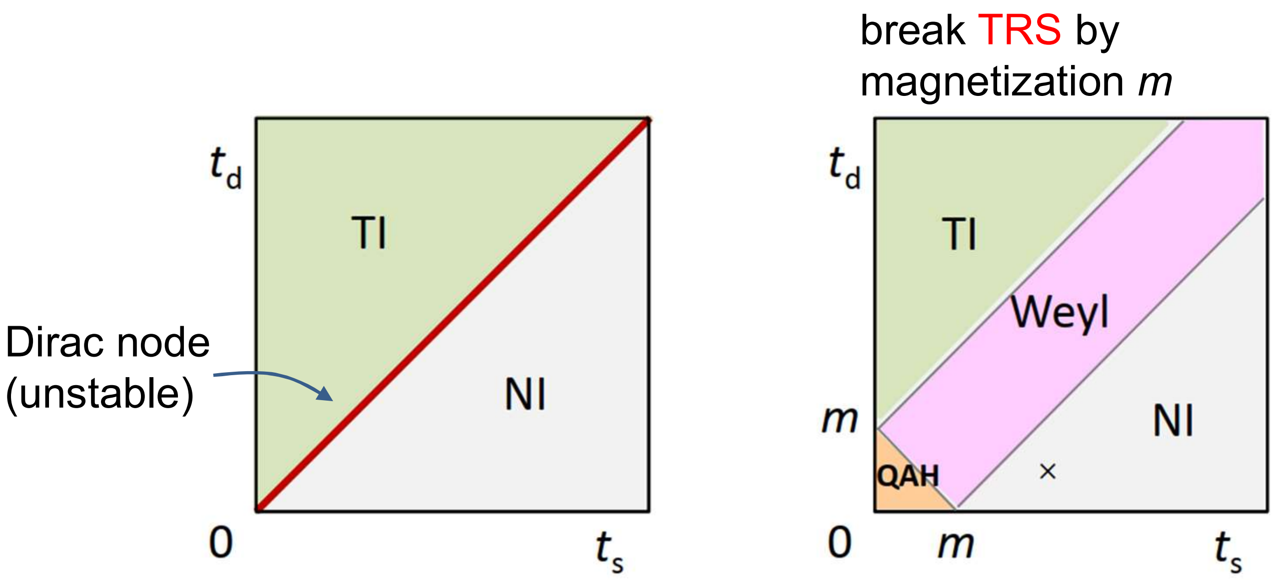

(a) m=0　　(b) $m\neq 0$

Weyl:

$$\underbrace{|t_S - t_D|}_{m_{c1}} < m < \underbrace{t_S + t_D}_{m_{c2}}$$

Anomalous QHE in Weyl SM

3D = a stack of 2D layers

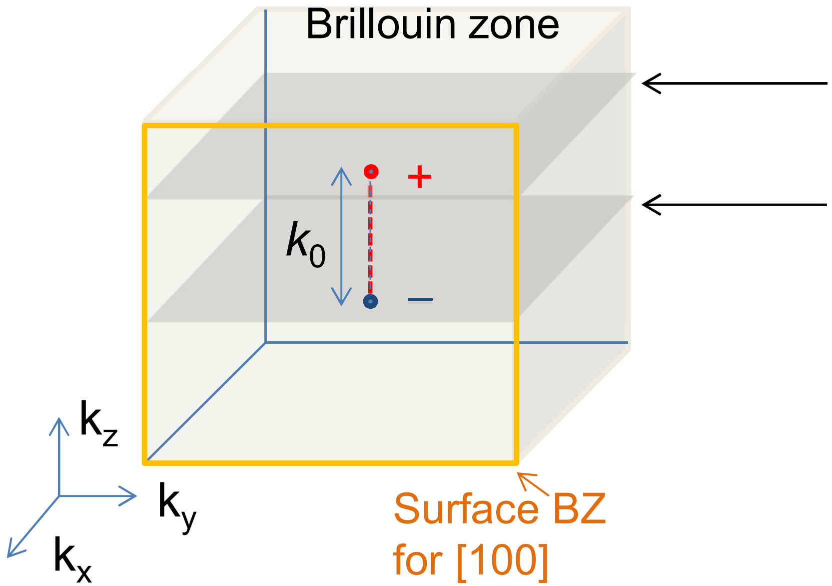

One 2D layer for each k_Z

Hall conductivity

$$\sigma_H^{2D}(k_z) = 0$$

$$\sigma_H^{2D}(k_z) = \frac{e^2}{h}$$

Cut through Dirac string (the center of vortex)

Total Hall conductivity

$$\sigma_H^{3D} = \frac{1}{L_z}\sum_{k_Z}\sigma_H^{2D}(k_Z) = \frac{e^2}{h}\frac{k_0}{2\pi}$$

- 2 Weyl nodes are created at origin
- They are linked by a string of gauge singularity (Dirac string)

Topological quantum properties of chiral crystals

Chiral crystals are materials with a lattice structure that has a well-defined handedness due to the lack of inversion, mirror or other roto-inversion symmetries. Although it has been shown that the presence of crystalline symmetries can protect topological band crossings, the topological electronic properties of chiral crystals remain largely uncharacterized. Here we show that Kramers–Weyl fermions are a universal topological electronic property of all non-magnetic chiral crystals with spin–orbit coupling and are guaranteed by structural chirality, lattice translation and time-reversal symmetry. Unlike conventional Weyl fermions, they appear at time-reversal-invariant momenta. We identify representative chiral materials in 33 of the 65 chiral space groups in which Kramers–Weyl fermions are relevant to the low-energy physics. We determine that all point-like nodal degeneracies in non-magnetic chiral crystals with relevant spin–orbit coupling carry non-trivial Chern numbers. Kramers–Weyl materials can exhibit a monopole-like electron spin texture and topologically non-trivial bulk Fermi surfaces over an unusually large energy window.

Kramers-Weyl point
with large Fermi arcs

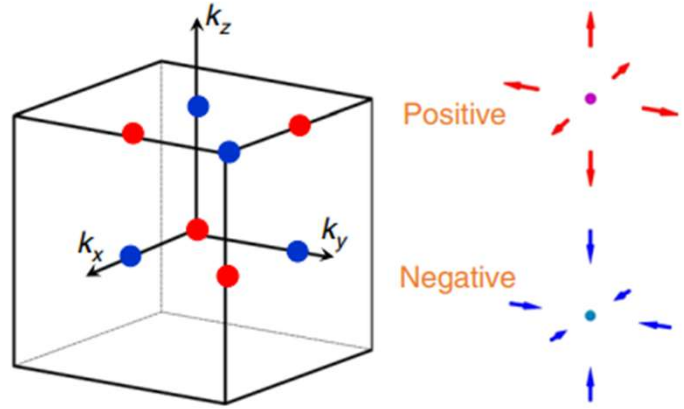

Chang et al, Nat Material 2018

Surface state and Fermi arc (Wan et al, PRB 2011)

2D Surface BZ for [100]

(Fermi level at Weyl node)

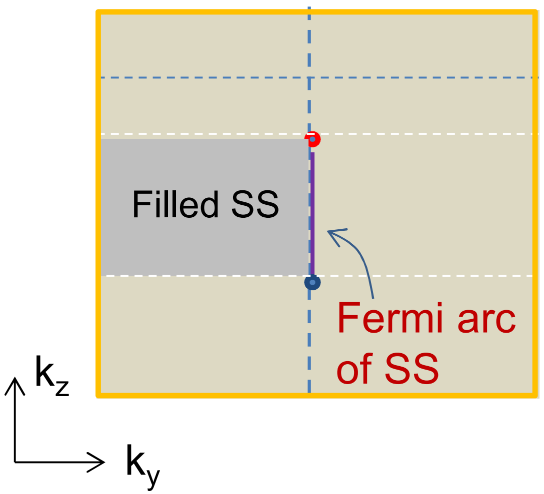

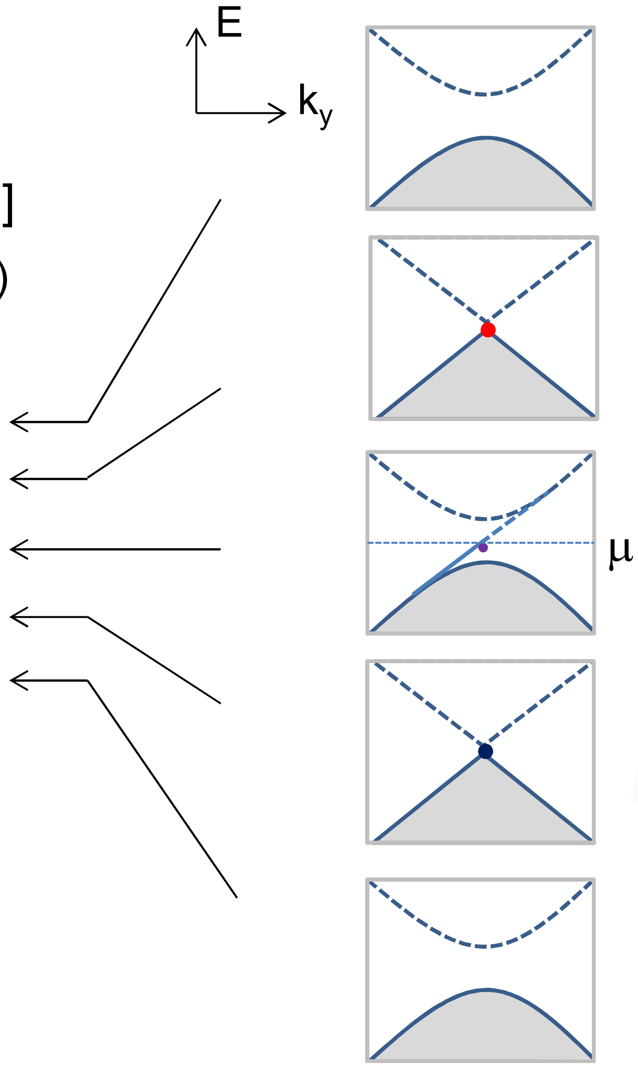

$\sigma_H^{2D}(k_z) = 0$

No edge state

Weyl point

$\sigma_H^{2D}(k_z) = \dfrac{e^2}{h}$

Chiral edge state of 2DEG

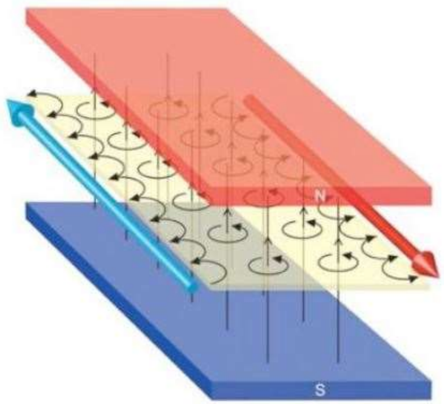

Weyl point and Fermi arc (3D view)

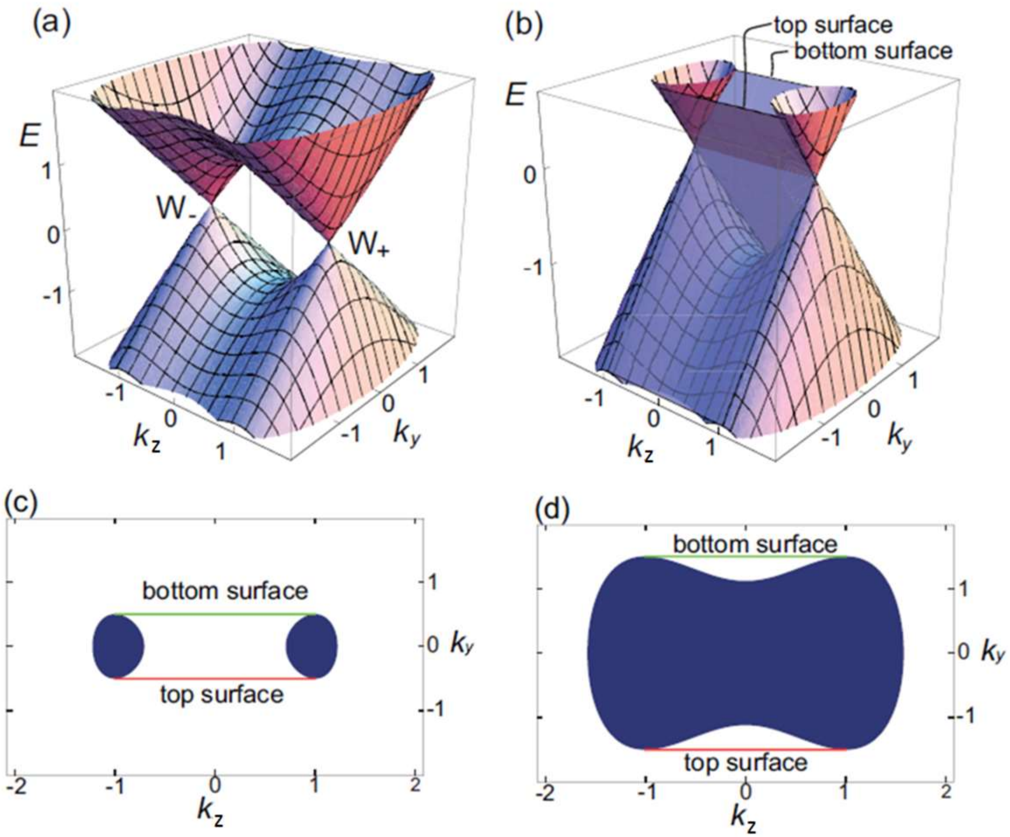

- SS connects to bulk states at Weyl nodes

Haldane 1401.0529

Surface Brillouin zone

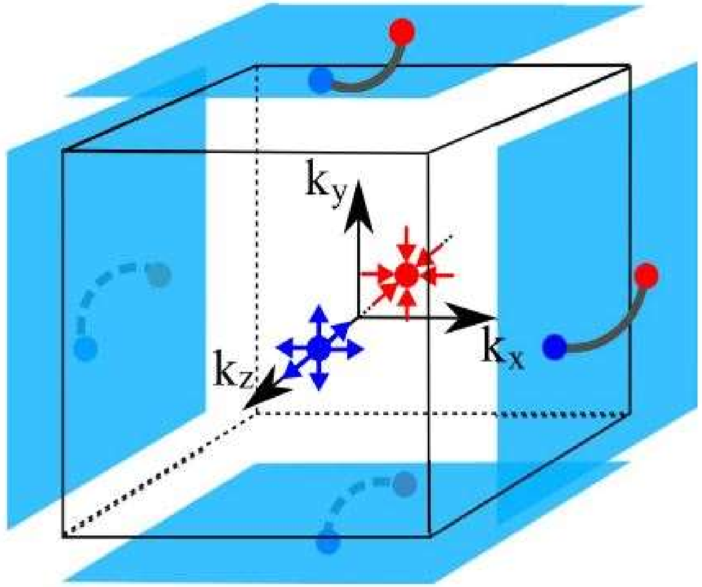

Fig from Kargarian et al, Sci Rep 2015

Fermi arc is impossible in pure 2D system

Fermi arc in
Transition metal monopnictide

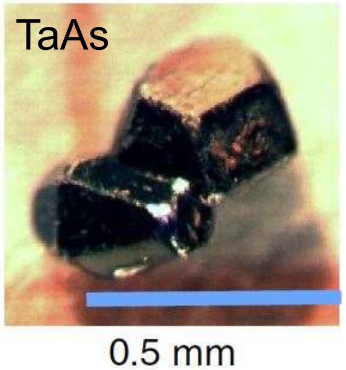

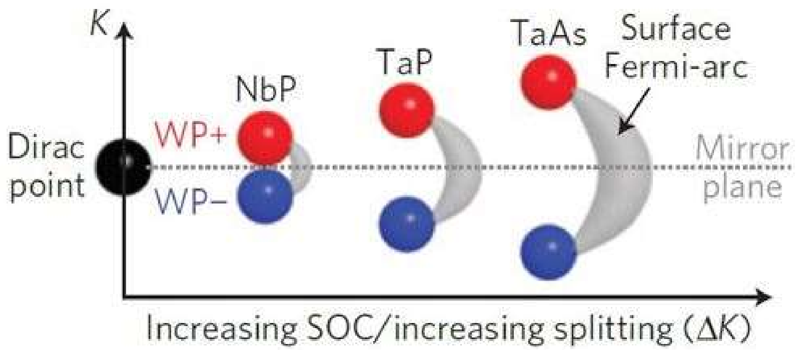

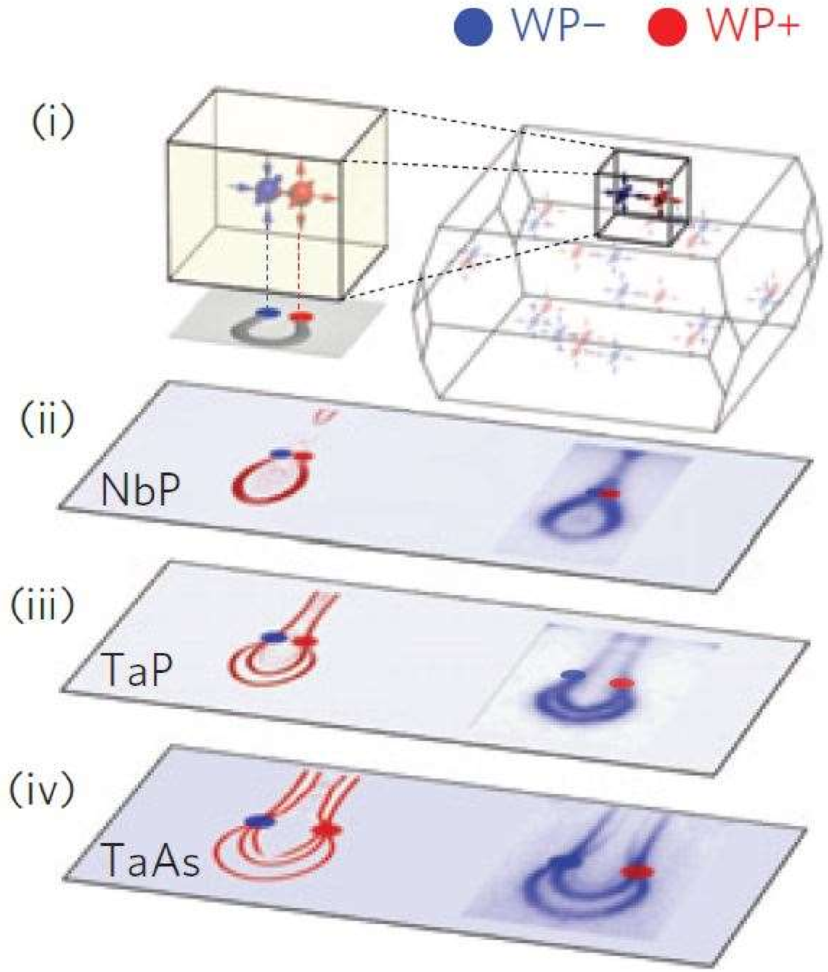

theory

experiment
(ARPES)

Z.K. Liu et al, Nature Material 2015

Weyl orbit

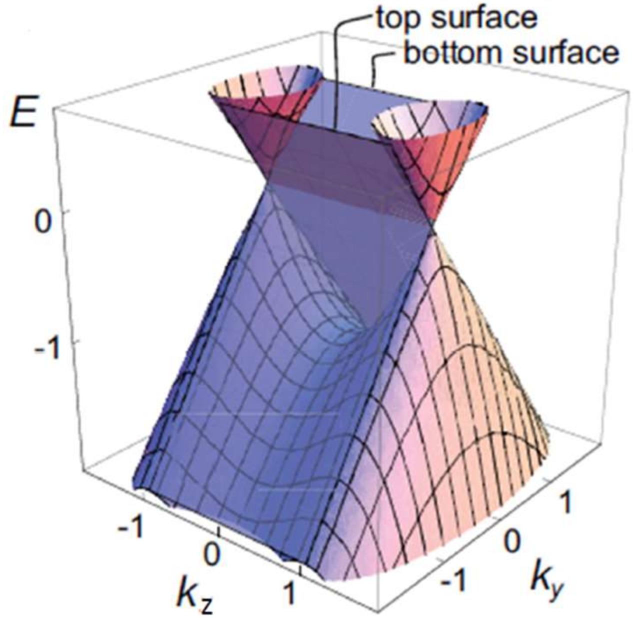

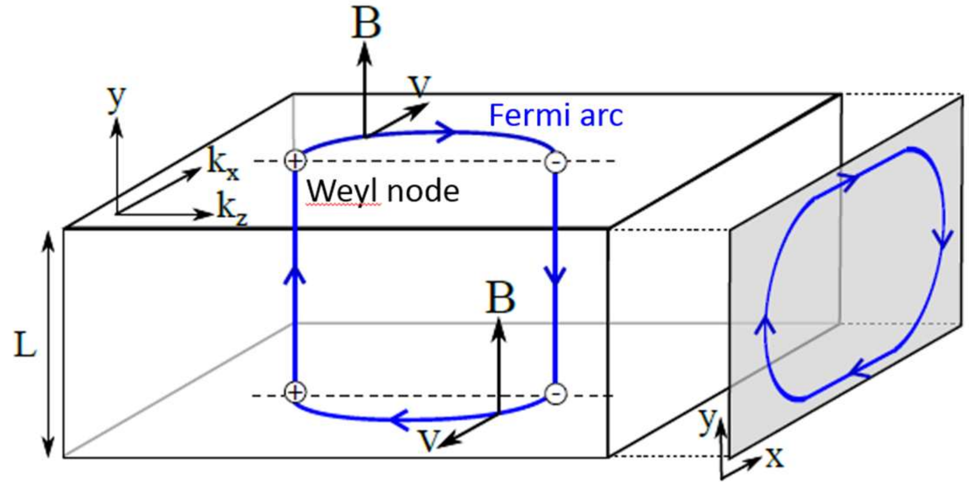

$$T = 2t_{arc} + 2t_{bulk}.$$

$$\varepsilon_n = (n+\delta)\frac{h}{T}, \;\; n = 0, 1, 2, \cdots$$

➡ De Haas-van Alphen oscillation

Potter, Kimchi, and Vishnawath, Nat Comm 2014